



# Development and characterization of camphor-loaded ozonated olive oil nanoemulsions

Tahir Emre YALÇIN<sup>1,2\*</sup> , Sevgi TAKKA<sup>1</sup> 

<sup>1</sup> Department of Pharmaceutical Technology, Faculty of Pharmacy, Gazi University, Yenimahalle 06330 Ankara, Turkey.

<sup>2</sup> Nano Farma Cosmetic Drug Consultancy Company, Gölbaşı 06830 Ankara, Turkey.

\* Corresponding Author. E-mail: emreyalcin@gazi.edu.tr (T.E.Y.); Tel. +90-312-202 30 41.

Received: 19 May 2020 / Revised: 17 July 2020 / Accepted: 10 August 2020

**ABSTRACT:** The purpose of present study is to prepare and characterize camphor-loaded ozonated olive oil nanoemulsions (NEs). In this study, olive oils were ozonated with different times (up to 24 h) and their viscosities were examined. NEs were prepared by high-energy ultrasonication technique and characterized according to droplet size distribution, zeta potential, microscopic evaluation, and storage stability. The effect of oil phase/aqueous phase volume ratio, sonication time, and co-solvent (glycerol) on formulations were evaluated. 6 h ozonated olive oil was chosen for developing NEs due to its liquid form and viscosity (189 mPas). The obtained camphor-loaded NEs (with or without glycerol) had nearly 300 nm droplet size with negative zeta potential. Microscopic analysis revealed the spherical shape of droplets. The long-term stability tests showed that camphor-loaded NEs with glycerol were more stable than NEs without glycerol at 4 °C and 25 °C. According to the results, ozonated olive oil based NEs with glycerol might be promising nanosystems for topical delivery of camphor.

**KEYWORDS:** Camphor; nanoemulsions; ozonated olive oil; long-term stability.

## 1. INTRODUCTION

In recent years, there has been a growing interest of ozone treatments. For the administration of ozone gas into the body, one of the effective and simple methods is to use ozonated oils [1]. Ozone is a very strong oxidative agent and has recently been utilized for the production of various forms of ozonated vegetable oils, which combines the properties of ozone and vegetable oils. It is a highly reactive molecule and easily reacts with carbon-carbon double bonds of unsaturated fatty acids that exist in triglycerides of vegetable oils in line with the mechanism defined by Criegee [2]. This reaction leads to a number of oxygenated products including ozonides, peroxides, and aldehydes [3]. These oxygenated compounds have several biological activities such as antibacterial, fungicidal and antiviral effect in addition to the properties of stimulating tissue regeneration and repair [4].

Musculoskeletal pain is a general health problem that affects people of all ages. Ozonated oils have been suggested as an alternative topical pain relief treatment due to their potential analgesic effect [5,6]. In this study, camphor was chosen as an active drug. It is an ingredient in topical analgesics and widely used to treat musculoskeletal pain in many ointments, creams, and gels. The combination of ozonated oils and camphor could be a good strategy for reducing musculoskeletal pain.

Nanocarriers, such as liposomes, transfersomes, ethosomes, niosomes, solid lipid nanoparticles, and nanoemulsions (NEs), are commonly used to improve skin penetration of active pharmaceutical ingredients. Among these drug delivery systems, NEs offer some advantages such as the controllable droplet size, long-term stability, and improved skin penetration for topical applications [7]. NEs are colloidal systems and have recently become important carriers as vehicles for both hydrophilic and hydrophobic substances in the wide range of applications for pharmaceutical and cosmetic products.

For developing ozonated oils based formulations, knowing the physicochemical features of ozonated oils plays a key role. The present study aims to emphasize the effect of ozonation time for olive oil and evaluate the effect of oil phase/aqueous phase volume ratio, sonication time, and co-solvent effect on formulation characteristics and long-term stability of NEs.

**How to cite this article:** Yalçin TE, Takka S. Development and characterization of camphor-loaded ozonated olive oil nanoemulsions. J Res Pharm. 2020; 24(6): 935-942.

## 2. RESULTS AND DISCUSSIONS

### 2.1. Characterization of ozonated vegetable oils

The first stage of this study was to determine optimum properties of ozonated olive oils to prepare NEs. The viscosity of oil phase is crucial for developing NEs because it affects the characteristic features. The effect of ozonation time on the viscosity of ozonated olive oils is illustrated in Figure 1. Results showed that the viscosity of ozonated oils increased during the ozonation time. Increased viscosity indicated that ozone reacted with the double bonds of the oil molecules to compose a more bulky molecule [8]. This result was in good agreement with the literature [9]. At the end of the 24 h, ozonized olive oils reached average viscosity value of 1833 mPas (Figure 1). On the other hand, the color of ozonated oils turned pale and lost their original colors and gained an almost colorless appearance as ozonation time increased (Figure 2). Changes may arise from the pronounced effect of ozone on carotenoid pigments which give their colors to the vegetable oils. The carotenoids show antioxidant activity [10] and have double carbon-carbon bonds [11]; therefore, they can be influenced by the reactions of ozonation. As a result of ozonation, the double carbon-carbon bonds of carotenoids can be broken and vegetable oils may lose their natural color.

Among the different time ozonated olive oils, 6 h ozonated olive oil was selected for NEs preparation. The following reasons were effective in this selection: (i) 9 h or higher ozonated olive oils were semi-solid and had high viscosity, which could make NEs preparation difficult and (ii) 3 h ozonated olive oil had low ozone content compared to 6 h.

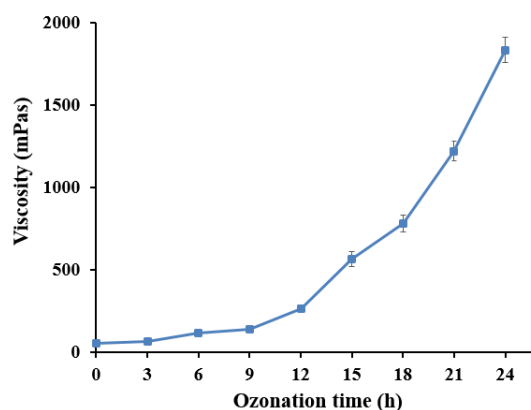


Figure 1. The change of ozonated olive oils viscosity with ozonation time at 25 °C (n=3).



Figure 2. The change in the appearance of ozonated olive oil within hours (A: Initial, B: 3 h, C: 6 h, D: 9 h, E: 12 h, F: 15 h, G: 18 h, H: 21 h, I: 24 h).

### 2.2. Characterization of NEs

#### 2.2.1. Effect of oil phase/aqueous phase volume ratio

The results of the influence of oil phase/aqueous phase volume ratio on nanoemulsion characteristics are summarized in Table 1. According to the results, it is clear that the droplet size and polydispersity index (PDI) value in NEs are influenced by the oil phase/aqueous phase volume ratio. The droplet size of NEs is growing with increasing volume of oil phase. The average droplet sizes of blank NEs were 3269 nm for low aqueous phase contained formulation (F1) and 297 nm for high aqueous phase contained formulation (F5). This result can be explained by decreasing viscosity of NEs with increasing aqueous phase volume. The decreased viscosity of NEs can make the fragmentation of the oil-water interface easy and result in the development of smaller droplets [12]. These observations are in accordance with similar studies. Kumar Dey

et al. reported that the average droplet size of NEs increased marginally with the increase in oil concentration [13]. Also Azeem et al. found that the droplet size increased with increase in the concentration of the oil in the formulations from 29.66 nm to 76.74 nm [14].

A high negative or positive value of zeta potential indicates a high electric charge on the surface of the NEs, which can cause strong electrostatic repulsion forces between droplets to prevent coalescence in order to maintain long-term physical stability. Both blank NEs exhibited negative zeta potentials in the range of -15.5 to -18.7 mV, which can be attributed to the presence of oleic acid in olive oil [15]. All formulations have high PDI value except F5. A small value of PDI (<0.5) indicates a narrow size distribution [16], while a large PDI (>0.7) indicates a very broad distribution of droplet size [17].

Droplet size plays an important role in skin penetration of NEs. NEs with a size  $\leq 300$  nm are able to deliver their contents into the deeper layers of the skin [18]. Therefore, it was decided that oil phase/aqueous phase volume ratio (1.5:8.5) was selected and used for further studies because of its high ozonated oil content and desired droplet size.

**Table 1.** Effects of different oil phase/aqueous phase volume ratio on the droplet characteristics of blank NEs (mean  $\pm$  SD, n=3).

Formulation code	Oil phase/aqueous phase ratio (v/v)	Particle size (nm)	PDI	Zeta potential (mV)
F1	7/3	3269 $\pm$ 352	1	-16.3 $\pm$ 1.2
F2	5/5	1340 $\pm$ 94	0.812 $\pm$ 0.064	-18.7 $\pm$ 0.9
F3	3/7	572 $\pm$ 10	0.516 $\pm$ 0.041	-15.5 $\pm$ 1.1
F4	2/8	432 $\pm$ 17	0.560 $\pm$ 0.063	-17.1 $\pm$ 1.0
F5	1.5/8.5	297 $\pm$ 5	0.440 $\pm$ 0.015	-16.9 $\pm$ 0.8

Applied sonication time is 5 min for all formulations.

### 2.2.2. Effect of sonication time on NEs

To evaluate the sonication time on formulation characteristics, different sonication times (2.5 min, 5 min, and 7.5 min) have been applied. The impact of sonication time on the droplet size and zeta potential of the blank NEs is presented in Figure 3A. These formulations (F5, F6, and F7) had similar oil phase/aqueous phase volume ratio (1.5:8.5); only the applied sonication times were different. Ultrasonication method has been employed in high energy emulsification to form intensive disruptive forces (such as collision and compression), which allows one phase to be dispersed into another as tiny droplets [19]. The result showed that droplet size was mainly dependent on the sonication time. Smaller droplets of NEs were formed with the increase in sonication time until 5 min. The average droplet size was obtained as 437 nm (F6), 297 nm (F5) and 302 nm (F7) at 2.5 min, 5 min, and 7.5 min sonication time, respectively. Partially larger droplets (with higher PDI value compared to F5) (Figure 3B) formed during longer sonication time (7.5 min) can be related to the effect of over-processing of the emulsification causing the coalescence of droplets [20]. These results are in line with the previous observations from the nanoemulsion formulations containing d-limonene. Jafari et al. reported that the size of NEs decreased when sonicated for up to 40 seconds, but when sonicated longer, the size remained constant in around 500 nm [21]. It is understood from the results that there is an optimum sonication time to obtain lower droplet size of NEs.

As shown in Figure 3A, all different sonication time applied formulations were negatively charged and zeta potential values varied between -15.4 mV and -16.9 mV.

### 2.2.3. Glycerol effect on NEs

The influence of a water-soluble co-solvent (glycerol) on the NEs was investigated. Statistical difference was only observed between F5 and F5G in terms of droplet size and formulation containing glycerol (F5G) had a larger droplet size and a higher PDI value compared to blank formulation (F5) (Table 2). F5G and F5 formulations were found to be 327  $\pm$  4 nm and 297  $\pm$  5 nm, respectively. This could be explained by the increase in viscosity of the aqueous phase with the presence of glycerol. The higher viscosity of NEs made it difficult to obtain smaller droplets [22]. All formulations were negative zeta potential with low PDI value (<0.5). Also, it was observed that the presence of glycerol in formulations did not significantly affect the zeta potential (p>0.05).

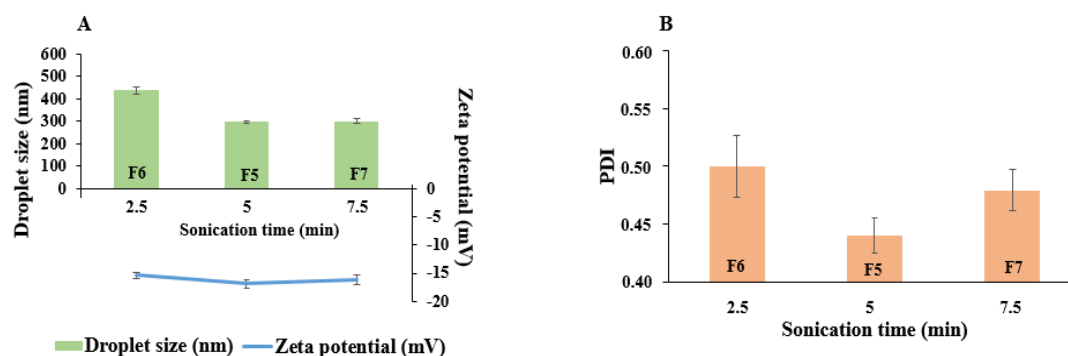


**Figure 3.** Effect of sonication time on (A) droplet size and zeta potential and (B) polydispersity index (PDI) (mean  $\pm$  SD, n=3).

**Table 2.** Characteristics of different NEs (mean  $\pm$  SD, n=3).

Formulation code	Droplet size (nm)	PDI	Zeta potential (mV)
F5	297 $\pm$ 5	0.440 $\pm$ 0.015	-16.9 $\pm$ 0.8
F5G	327 $\pm$ 4*	0.452 $\pm$ 0.017	-16.6 $\pm$ 0.4
F5C	315 $\pm$ 11	0.460 $\pm$ 0.028	-17.9 $\pm$ 0.9
F5GC	305 $\pm$ 12	0.495 $\pm$ 0.011	-17.3 $\pm$ 0.7

Difference between F5 and F5G, \* p<0.05.  
F5: Blank NEs (without glycerol and camphor)  
F5G: NEs containing glycerol (without camphor)  
F5C: NEs containing camphor (without glycerol)  
F5GC: NEs containing glycerol and camphor

#### 2.2.4. Microscopic evaluation of the NEs

Figure 4 shows microscopic images of camphor-loaded NEs with or without glycerol. All emulsions showed spherical droplets. The NEs droplets remained dispersed by microscopy images, which could be attributed to the preparation method (high-energy ultrasonication technique) [23].

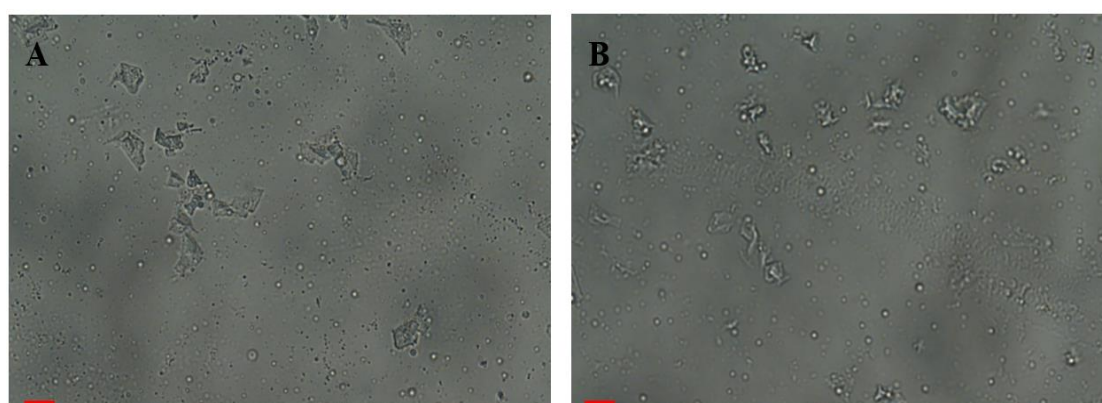


**Figure 4.** Optical microscopic images of (A) camphor-loaded NEs with glycerol and (B) camphor-loaded NEs without glycerol. Scale bar corresponds to 8  $\mu$ m.

### 2.2.5. Storage stability of NEs

For commercial applications, it is an important factor that emulsion-based delivery systems remain physically stable during storage. The long-term stability of camphor-loaded NEs with glycerol (F5GC) or without glycerol (F5C) in terms of droplet size, PDI and zeta potential were monitored at 4 °C, 25 °C ± 2 °C, and 40 °C ± 2 °C. The results showed that the stability of NEs was highly influenced by the storage temperature and presence of glycerol (Table 3). Statistically, the droplet size of the F5GC showed physical stability for a period of 6 months ( $p > 0.05$ ); however, in the absence of glycerol, F5C showed stability for just a period of 3 months at 4 °C. By the end of 6 months, at 25 °C, the droplet size increased to 351 nm and 378 nm for F5GC and F5C, respectively. It was found that after 1 month storage, droplet size slightly increased at 40 °C in both formulations ( $p < 0.05$ ). The mean droplet size of the F5C and F5GC increased to about 494 nm and 443 nm at 40°C, respectively, in 6 months possibly due to aggregation [24,25]. This also demonstrated the low stability of NEs at 40 °C as a result of coalescence and aggregation. Although formulation F5GC had low PDI values ( $< 0.5$ ) in all conditions, F5C showed higher PDI values especially when formulations were stored at 40 °C for a long time. Because of several diverse physicochemical procedures involving flocculation, coalescence, and Ostwald ripening under stress conditions (such as high temperature and high humidity), NEs may get unstable [26]. By adding glycerol, physical stability of the NEs was significantly enhanced, due to its co-solvent and extremely viscous property. With increasing the viscosity of the continuous phase droplet collision frequency was decreased [27]. Also, NEs formulations (with or without glycerol) had a negative zeta potential during all storage conditions.

**Table 3.** Changes in the droplet size (nm), PDI and zeta potential (mV) of camphor-loaded NEs during storage time at different conditions (mean ± SD, n=3).

Time (Months)	Conditions	Droplet size (nm)		PDI		Zeta potential (mV)	
		F5C	F5GC	F5C	F5GC	F5C	F5GC
Initial		315 ± 11	305 ± 12	0.460 ± 0.028	0.495 ± 0.011	-17.9 ± 0.9	-17.3 ± 0.7
	4 °C	333 ± 11	321 ± 8	0.465 ± 0.033	0.381 ± 0.038	-18.2 ± 0.6	-17.3 ± 0.9
1	25 °C ± 2 °C	333 ± 17	314 ± 10	0.457 ± 0.034	0.425 ± 0.032	-16.4 ± 0.9	-18.4 ± 0.5
	40 °C ± 2 °C	350 ± 8	321 ± 10	0.533 ± 0.016	0.397 ± 0.029	-18.1 ± 0.7	-18.3 ± 0.9
	4 °C	340 ± 15	325 ± 6	0.507 ± 0.047	0.438 ± 0.007	-18.3 ± 1.1	-16.1 ± 0.6
3	25 °C ± 2 °C	359 ± 9	330 ± 11	0.476 ± 0.038	0.431 ± 0.022	-18.9 ± 0.8	-17.7 ± 1.1
	40 °C ± 2 °C	385 ± 16	360 ± 12	0.568 ± 0.061	0.421 ± 0.035	-17.6 ± 1.0	-17.3 ± 0.7
	4 °C	355 ± 13	330 ± 14	0.572 ± 0.065	0.454 ± 0.030	-18.1 ± 0.9	-16.8 ± 0.9
6	25 °C ± 2 °C	378 ± 11	351 ± 9	0.661 ± 0.084	0.487 ± 0.018	-16.2 ± 0.5	-17.4 ± 1.1
	40 °C ± 2 °C	494 ± 40	443 ± 13	0.604 ± 0.059	0.482 ± 0.017	-17.3 ± 0.7	-16.1 ± 0.8

### 3. CONCLUSION

There are a number of major parameters (such as ozonation time, unsaturated fatty acids ratio and monounsaturated fats/polyunsaturated fats ratio) which can change the physicochemical properties of ozonated oils. Amongst ozonated olive oils, 6 h ozonated olive oil showed excellent properties for preparing NEs formulations. The camphor-loaded NEs were prepared using high energy emulsification method (ultrasonication) and successfully characterized in vitro. Spherical droplets with average sizes around 300 nm were prepared with negative zeta potential. It was obvious that glycerol played a major role for the stability of the emulsions. According to droplet size analyzer results, glycerol included NEs appear to be more stable at all storage conditions except 40 °C. In conclusion, nanoemulsion based gel (nano-emulgel), which exhibits complementary characteristics of NEs and gels, can be a new alternative strategy for the delivery of camphor in ozonated oil based NEs for both in vitro and in vivo further investigations.

## 4. MATERIALS AND METHODS

### 4.1. Materials

Olive oil was purchased from the local companies in Turkey. Tween 20 (surfactant), glycerol (co-solvent), and camphor were purchased from Sigma-Aldrich (USA). Water used in the experiment was distilled.

### 4.2. Ozonation method

Ozonated olive oil was prepared as shown in Figure 5. Ozone was generated by the ozone generator (Elite Ozon, Turkey). The oxygen required for ozone generation was provided from oxygen concentrator. Pure oils were placed in a reactor at room temperature. The ozone (gas flow rate: 1.5 l/min) was bubbled through the oil samples for different periods of time up to 24 h.

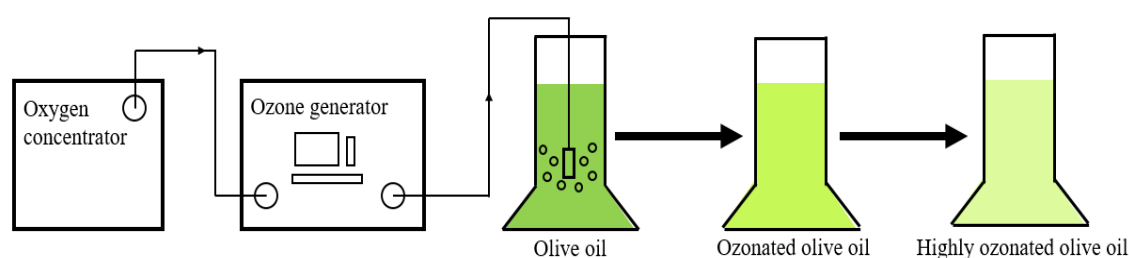


**Figure 5.** Scheme of the preparation of ozonated olive oil. The olive oil begins to lose their original colors with increasing ozonation time.

### 4.3. Characterization of ozonated olive oil

The viscosity measurement was performed with a viscometer (Brookfield model LV-DVIII, USA, spindle CPE-52) at different temperatures. The sample (0.5 ml) was placed between the gap of the cone and plate, and the gap was closed gradually. Revolving speed was 10 rpm.

### 4.4. Preparation of NEs

A high-energy ultrasonication technique was used to prepare the NEs [28]. Briefly, 2.5% (v/v) tween 20 and 2.5% (v/v) glycerol were dissolved in distilled water (aqueous phase). The oil phase was prepared by adding camphor into the ozonated olive oil. The oil phase and aqueous phase were stirred separately with a magnetic stirrer for 30 min to get homogeneous solutions. The oil phase was added slowly to the aqueous phase and mixed with a magnetic stirrer for 30 min in order to get a coarse emulsion. Afterwards, the coarse emulsion was sonicated (Sonics Vibra-Cell, USA) to get the NEs. The blank formulations were prepared as described above without camphor. The general scheme for the preparation of NEs is shown in Figure 6. The effect of formulation variables such as oil phase/aqueous phase volume ratio, sonication time, and co-solvent effect on NEs characteristics were evaluated.

### 4.5. Characterization of NEs

#### 4.5.1. Zeta potential, droplet size and polydispersity index analyses

All formulations were characterized for the zeta potential, droplet size, and PDI using a Malvern ZetaSizer Nano ZS instrument (Malvern Instruments, UK). The surface charge measurements were based on the electrophoretic mobility of NEs and the droplet size and PDI of NEs were determined by Dynamic Light Scattering (DLS) technique. All determinations were performed in triplicate (n=3).

#### 4.5.2. Microscopic evaluation of the NEs

The microscopic and structural depiction of the NEs was scrutinized. Optical microscopy images were recorded by an optical microscope (Olympus IX53, Japan) to analyze the morphology of NEs. A drop of nanoemulsion samples were dispersed on the glass slide and samples were then covered with the coverslip. Images were observed under the microscope with an objective lens of 100× magnification power.

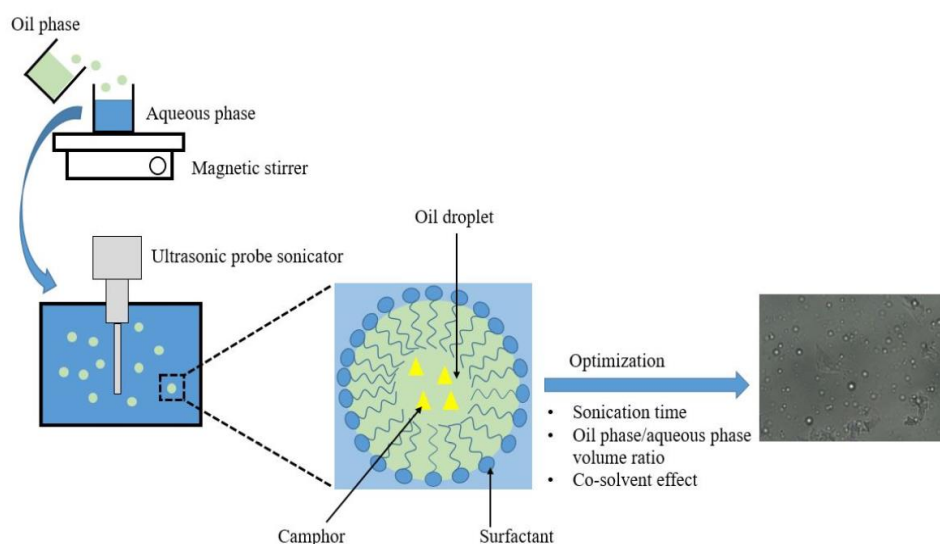


**Figure 6.** Schematic preparation of NEs.

#### 4.5.3. Determination of storage stability of NEs

In order to evaluate storage stability of the NEs, the samples were put into capped glass containers and stored at 4 °C, 25 °C ± 2 °C (60% RH) and 40 °C ± 2 °C (75% RH) for 6 months in a stability chamber. The storage stability of the NEs was determined by testing their droplet size, PDI, and zeta potential during storage (n=3).

#### 4.6. Statistical analysis

All data were collected from triplicates (n=3) and were reported as the average with standard deviation (mean ± SD). All analyses were performed using GraphPad Prism 5.0 (GraphPad Software Inc.). Data were analyzed using one-way ANOVA with post-hoc Tukey's test. A difference with  $p < 0.05$  was considered to be statistically significant.

**Acknowledgements:** The Scientific and Technological Research Council of Turkey (TUBITAK) with a grant number 2170573 supported this work. The author (T.E.Y.) would like to thank Yuksel Yalcin for his helps to complete this project.

**Author contributions:** Concept – T.E.Y., S.T.; Design – T.E.Y., S.T.; Supervision – S.T.; Resources – T.E.Y.; Materials – T.E.Y.; Data Collection and/or Processing – T.E.Y.; Analysis and/or Interpretation – T.E.Y.; Literature Search – T.E.Y.; Writing – T.E.Y.; S.T.; Critical Reviews – T.E.Y.; S.T.

**Conflict of interest statement:** The authors declared no conflict of interest" in the manuscript.

#### REFERENCES

- [1] Valacchi G, Fortino V, Bocci V. The dual action of ozone on the skin. *Br J Dermatol.* 2005; 153(6): 1096-1001. [\[CrossRef\]](#)
- [2] Sega A, Zanardi I, Chiasserini L, Gabbrielli A, Bocci V, Travagli V. Properties of sesame oil by detailed 1H and 13C NMR assignments before and after ozonation and their correlation with iodine value, peroxide value, and viscosity measurements. *Chem Phys Lipids.* 2010; 163(2): 148-156. [\[CrossRef\]](#)
- [3] Sadowska J, Johansson B, Johannessen E, Friman R, Broniarz-Press L, Rosenholm JB. Characterization of ozonated vegetable oils by spectroscopic and chromatographic methods. *Chem Phys Lipids.* 2008; 151(2): 85-91. [\[CrossRef\]](#)
- [4] Song M, Zeng Q, Xiang Y, Gao L, Huang J, Huang J, Wu K, Lu J. The antibacterial effect of topical ozone on the treatment of MRSA skin infection. *Mol Med Rep.* 2018; 17(2): 2449-2455. [\[CrossRef\]](#)
- [5] El Hadary AA, Yassin HH, Mekhemer ST, Holmes JC, Grootveld M. Evaluation of the effect of ozonated plant oils on the quality of osseointegration of dental implants under the influence of cyclosporin a: an in vivo study. *J Oral Implantol.* 2011; 37(2): 247-257. [\[CrossRef\]](#)
- [6] Currò M, Russo T, Ferlazzo N, Caccamo D, Antonuccio P, Arena S, Parisi S, Perrone P, Ientile R, Romeo C, Impellizzeri P. Anti-inflammatory and tissue regenerative effects of topical treatment with ozonated olive oil/vitamin E acetate in balanitis xerotica obliterans. *Molecules.* 2018; 23: 645. [\[CrossRef\]](#)

- [7] Rai VK, Mishra N, Yadav KS, Yadav NP. Nanoemulsion as pharmaceutical carrier for dermal and transdermal drug delivery: Formulation development, stability issues, basic considerations and applications. *J Control Release*. 2018; 270: 203-225. [\[CrossRef\]](#)
- [8] John J, Bhattacharya M, Raynor PC. Emulsions containing vegetable oils for cutting fluid application. *Colloids Surf A Physicochem Eng Asp*. 2004; 237(1): 141-150. [\[CrossRef\]](#)
- [9] Guerra-Blanco P, Poznyak T, Chairez I, Brito-Arias M. Correlation of structural characterization and viscosity measurements with total unsaturation: An effective method for controlling ozonation in the preparation of ozonated grape seed and sunflower oils. *Eur J Lipid Sci Tech*. 2015; 117(7): 988-998. [\[CrossRef\]](#)
- [10] Stahl W, Sies H. Antioxidant activity of carotenoids. *Mol Aspects Med*. 2003; 24(6): 345-351. [\[CrossRef\]](#)
- [11] Benevides CMdJ, Veloso MCdC, de Paula Pereira PA, Andrade JBd. A chemical study of  $\beta$ -carotene oxidation by ozone in an organic model system and the identification of the resulting products. *Food Chem*. 2011; 126(3): 927-934. [\[CrossRef\]](#)
- [12] Mehmood T, Ahmad A, Ahmed A, Ahmed Z. Optimization of olive oil based O/W nanoemulsions prepared through ultrasonic homogenization: A response surface methodology approach. *Food Chem*. 2017; 229: 790-796. [\[CrossRef\]](#)
- [13] kumar Dey T, Ghosh S, Ghosh M, Koley H, Dhar P. Comparative study of gastrointestinal absorption of EPA & DHA rich fish oil from nano and conventional emulsion formulation in rats. *Food Res Int*. 2012; 49(1): 72-79. [\[CrossRef\]](#)
- [14] Azeem A, Rizwan M, Ahmad FJ, Iqbal Z, Khar RK, Aqil M, Talegaonkar S. Nanoemulsion components screening and selection: a technical note. *AAPS PharmSciTech*. 2009; 10(1): 69-76. [\[CrossRef\]](#)
- [15] Karami Z, Khoshkam M, Hamidi M. Optimization of olive oil-based nanoemulsion preparation for intravenous drug delivery. *Drug Res (Stuttg)*. 2019; 69(5): 256-264. [\[CrossRef\]](#)
- [16] Md S, Gan SY, Haw YH, Ho CL, Wong S, Choudhury H. In vitro neuroprotective effects of naringenin nanoemulsion against  $\beta$ -amyloid toxicity through the regulation of amyloidogenesis and tau phosphorylation. *Int J Biol Macromol*. 2018; 118: 1211-1219. [\[CrossRef\]](#)
- [17] Gharibzahedi SMT, Mohammadnabi S. Effect of novel bioactive edible coatings based on jujube gum and nettle oil-loaded nanoemulsions on the shelf-life of Beluga sturgeon filets. *Int J Biol Macromol*. 2017; 95: 769-777. [\[CrossRef\]](#)
- [18] Hanifah M, Jufri M. Formulation and Stability Testing of Nanoemulsion Lotion Containing Centella asiatica Extract. *J Young Pharm*. 2018; 10(4): 404-408. [\[CrossRef\]](#)
- [19] Azmi NAN, Elgharbawy AAM, Motlagh SR, Samsudin N, Salleh HM. Nanoemulsions: Factory for Food, Pharmaceutical and Cosmetics. *Processes*. 2019; 7(9): 617. [\[CrossRef\]](#)
- [20] Lu W-C, Chiang B-H, Huang D-W, Li P-H. Skin permeation of d-limonene-based nanoemulsions as a transdermal carrier prepared by ultrasonic emulsification. *Ultrason Sonochem*. 2014; 21(2): 826-832. [\[CrossRef\]](#)
- [21] Jafari SM, He Y, Bhandari B. Nano-emulsion production by sonication and microfluidization-a comparison. *Int J Food Prop*. 2006; 9(3): 475-485. [\[CrossRef\]](#)
- [22] Li Y, Jin H, Sun X, Sun J, Liu C, Liu C, Xu J. Physicochemical Properties and Storage Stability of Food Protein-Stabilized Nanoemulsions. *Nanomaterials (Basel)*. 2018; 9(1): 25. [\[CrossRef\]](#)
- [23] Tang SY, Shridharan P, Sivakumar M. Impact of process parameters in the generation of novel aspirin nanoemulsions - Comparative studies between ultrasound cavitation and microfluidizer. *Ultrason Sonochem*. 2013; 20(1): 485-497. [\[CrossRef\]](#)
- [24] Yalçın TE, Ilbasımis-Tamer S, Takka S. Development and characterization of gemcitabine hydrochloride loaded lipid polymer hybrid nanoparticles (LPHNs) using central composite design. *Int J Pharm*. 2018; 548(1): 255-262. [\[CrossRef\]](#)
- [25] Yalçın TE, Ilbasımis-Tamer S, Ibisoglu B, Özdemir A, Ark M, Takka S. Gemcitabine hydrochloride-loaded liposomes and nanoparticles: comparison of encapsulation efficiency, drug release, particle size, and cytotoxicity. *Pharmaceutical Development and Technology*. 2018; 23(1): 76-86. [\[CrossRef\]](#)
- [26] Saberi AH, Fang Y, McClements DJ. Effect of glycerol on formation, stability, and properties of vitamin-E enriched nanoemulsions produced using spontaneous emulsification. *J Colloid Interface Sci*. 2013; 411: 105-113. [\[CrossRef\]](#)
- [27] Sakulku U, Nuchuchua O, Uawongyart N, Puttipatkhachorn S, Soottitawat A, Ruktanonchai U. Characterization and mosquito repellent activity of citronella oil nanoemulsion. *Int J Pharm*. 2009; 372(1): 105-111. [\[CrossRef\]](#)
- [28] Thakkar HP, Khunt A, Dhande RD, Patel AA. Formulation and evaluation of Itraconazole nanoemulsion for enhanced oral bioavailability. *J Microencapsul*. 2015; 32(6): 559-569. [\[CrossRef\]](#)

This is an open access article which is publicly available on our journal's website under Institutional Repository at <http://dSPACE.marmara.edu.tr>.